Determination of spin-exchange parameters between optically pumped rubidium and ^{83}Kr

S. R. Schaefer, G. D. Cates, and W. Happer
Department of Physics, Princeton University, Princeton, New Jersey 08544
(Received 5 January 1990)

The spin-exchange rates due to binary collisions and due to the formation of van der Waals molecules between ^{83}Kr nuclei and optically pumped rubidium-metal vapor have been determined using a technique that relies on the simultaneous observation of frequency shifts of nuclear magnetic resonance lines of noble-gas atoms and corresponding frequency shifts of electron paramagnetic resonance lines of alkali-metal atoms. In contrast, earlier studies have relied on the observation of the spin-relaxation rate of either the alkali-metal atoms or the noble-gas atoms.

I. INTRODUCTION

The nuclei of noble-gas can be polarized by spin exchange with optically pumped alkali-metal vapor.[1,2] This technique has become increasingly popular due to its simplicity and the long spin-relaxation times associated with nuclear polarized noble gases. In atomic physics, experiments utilizing spin exchange in alkali-metal–noble-gas systems have included studies of quadrupolar-wall interactions,[3] tests of local Lorentz invariance,[4] and searches for permanent electric-dipole moments in atoms.[5] In nuclear physics, applications of spin exchange have included the measurement of the magnetic moments of a wide variety of radioactive noble-gas isotopes,[6] and the production of polarized targets.[7] Other novel applications of spin exchange have included using a sample of polarized ^{3}He as a "spin filter" to polarize epithermal neutrons for the study of parity-violating neutron absorption resonances,[8] and a recent proposal to stop unpolarized negative muons in polarized noble gases in an effort to create polarized muonic atoms.[9] Clearly, in addition to being interesting to study for its own sake, spin exchange in alkali-metal–noble-gas systems has become increasingly useful in a variety of contexts, making the characterization of spin-exchange processes quite interesting.

We report here the first measurement of the spin-exchange rates due to binary collisions and due to the formation of van der Waals molecules between ^{83}Kr nuclei (which have a nuclear spin $K=\frac{9}{2}$) and optically pumped rubidium-metal vapor. We have used a technique for our studies that is based on the observation of frequency shifts of the nuclear magnetic resonance (NMR) lines of the noble-gas nuclei and the electron paramagnetic resonance (EPR) lines of the alkali-metal atoms. As was first shown by Grover,[10] the spin-polarized nuclei of noble-gas atoms causes a shift in the EPR frequency of the alkali-metal atoms when both types of atoms are in the same gaseous sample. Similarly, the spin-polarized valence electrons of the alkali-metal atoms causes a shift of the NMR frequency of noble gases. These shifts have been described extensively by Schaefer *et al.* in an earlier paper.[11] Prior to this work, the study of spin-relaxation times has provided the primary means of investigating spin exchange in alkali-metal–noble-gas systems. However, because of the ^{83}Kr nucleus interacts so weakly with the Rb atom, the Rb-induced nuclear relaxation rate of ^{83}Kr is quite small compared to the wall-induced relaxation rate at the highest Rb vapor pressures for which our optical probing methods can be used. Furthermore, the wall relaxation rate is temperature dependent, thus complicating measurements in which the Rb vapor pressure is temperature controlled. It is consequently very difficult to use studies of ^{83}Kr nuclear spin-relaxation rates to determine the basic spin interaction coupling constants of the Rb-^{83}Kr system while still employing optical probing of the nuclear polarization. We have therefore used the new frequency-shift method described below to determine the coupling constants. The walls have no influence on the frequency shift, except indirectly, in that wall-induced relaxation limits the ultimate polarization that can be produced in the sample. By making our measurements at a single temperature, the effect of the walls on the ^{83}Kr polarization was held constant. The technique of frequency shifts has the advantage that frequencies can be measured quite accurately. Also, it has the advantage that systematic errors associated with knowing accurately the alkali-metal number density are suppressed. The disadvantage of the technique is that interpreting the data requires prior knowledge of κ_0, an enhancement parameter, previously measured[11] by Schaefer *et al.*, that appears in the equations that describe the frequency shifts [see Eq. (29), for instance]. Fortunately, the dependence of our data on κ_0 is suppressed, as will be discussed later.

To illustrate the technique, a representative measurement is shown in Fig. 1. Each data point represents a measurement of the nuclear polarization of a ^{83}Kr sample that has been polarized by spin exchange with optically pumped Rb vapor. The ^{83}Kr polarization is measured by observing the shift it causes in the EPR frequency of the Rb vapor. An oscillating magnetic field, near the Larmor frequency of ^{83}Kr, is applied to the sample while it is being polarized. When the frequency is near resonance, the buildup of polarization is inhibited. By observing the final ^{83}Kr polarization as a function of the frequency of

the oscillating magnetic field, the NMR lines shown in Fig. 1 are obtained. The upper and lower NMR lines correspond to the Rb vapor being polarized antiparallel and parallel to the magnetic field, respectively. The shift between the two NMR lines is due to the effective magnetic field created by the polarized Rb vapor. More details concerning Fig. 1 appear in the experimental section.

At pressures below about 150 Torr, spin exchange in the Rb-Kr system takes place mostly in loosely bound van der Waals molecules that are formed during collisions between a Rb atom, a Kr atom, and a third body.[1,2,12] The simplest spin Hamiltonian for the Rb-Kr system consistent with presently known experimental data is

$$H = A\mathbf{I}\cdot\mathbf{S}+\gamma\mathbf{N}\cdot\mathbf{S}+\alpha\mathbf{K}\cdot\mathbf{S}+g_S\mu_B\cdot\mathbf{S}+\cdots, \quad (1)$$

where $A\mathbf{I}\cdot\mathbf{S}$ is the hyperfine interaction between the alkali-metal valence electron spin $\mathbf{S}$ and its own nuclear spin $\mathbf{I}$, $\gamma\mathbf{N}\cdot\mathbf{S}$ is the spin-rotation interaction between $\mathbf{S}$ and the rotational angular momentum $\mathbf{N}$ of the Rb-Kr system, $\alpha\mathbf{K}\cdot\mathbf{S}$ is the Fermi contact interaction between $\mathbf{S}$ and the nuclear spin $\mathbf{K}$ of the Kr, and $g_s\mu_B\mathbf{B}\cdot\mathbf{S}$ is the largest of the Zeeman terms. We note that the term $\alpha\mathbf{K}\cdot\mathbf{S}$ is responsible for spin exchange in the Rb-Kr system. The spin-rotation interaction $\gamma\mathbf{N}\cdot\mathbf{S}$ is the primary cause of the spin relaxation of optically pumped Rb vapor in the Rb-Kr system, and has been measured previously by Bouchiat, Brossel, and Pottier.[12] A full determination of the Rb-Kr, system requires an understanding of each of the terms in (1). Also, one must characterize the formation and breakup rates of the van der Waals molecules, and their mean molecular lifetime τ.

Three quantities are measured in our experiment: the ^{85}Rb EPR shift $\Delta\nu(^{85}\mathrm{Rb})$, the ^{83}Kr NMR shift $\Delta\nu(^{83}\mathrm{Kr})$, and the longitudinal relaxation rate of the ^{83}Kr nuclear polarization Γ, due largely to wall collisions. Representative examples of the raw data obtained in our experiment are shown in Figs. 1 and 2. The ^{83}Kr NMR shift is one-half of the splitting between the two NMR lines that appear in Fig. 1. A measurement of the longitudinal spin-relaxation rate Γ is shown in Fig. 2, in which the EPR shift is graphed as a function of time, illustrating the exponential decay of the Rb EPR shift which is proportional to $\langle K_z\rangle$. The measurement of $\Delta\nu(^{85}\mathrm{Rb})$, that appears in (2) below, is illustrated in both Figs. 1 and 2. The quantity $\Delta\nu(^{85}\mathrm{Rb})$ is defined here as the *maximum* EPR shift that is obtained when a cell is pumped with a given laser power for a set length of time. In Fig. 2, it is the initial EPR shift that occurs before the ^{83}Kr polarization begins to decay. In Fig. 1, it corresponds to the base line of the NMR lines, that is, the EPR shift that is obtained when the applied oscillating magnetic field is sufficiently far from resonance that the buildup of Kr polarization is not inhibited. We will show that the product of the ratio of the frequency shifts and Γ can be written

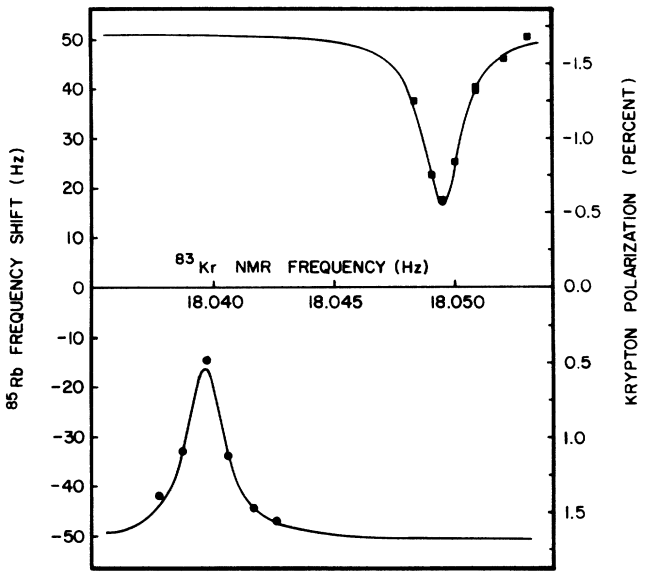

FIG. 1. Nuclear magnetic resonance (NMR) scan for ^{83}Kr. For the lower resonance curve, $\langle S_z\rangle$ and $\langle K_z\rangle$ are parallel to the external magnetic field B, and for the upper curve $\langle S_z\rangle$ and $\langle K_z\rangle$ are antiparallel to the external field. The nuclear resonance appears as a shift of the electron paramagnetic resonance (EPR) frequency. As discussed in the text, the EPR frequency shift is directly proportional to the nuclear spin polarization of the Kr atoms. The scale for the krypton polarization (defined here as $\langle K_z\rangle/K$) is subject to a 33% uncertainty in the Rb polarization. The width of the curves is dominated by the small splitting of the ^{83}Kr spin sublevels by the interaction of the nuclear quadrupole moment with an electric field gradient, which acts on the nucleus while the Kr atom is close to the surface of the sample cell.

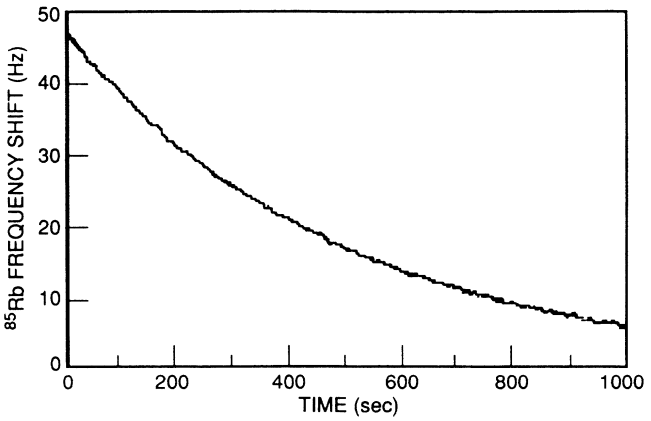

FIG. 2. The ^{85}Rb EPR shift, which is proportional to $\langle K_z\rangle$, is plotted as a function of time. Data of this sort are used to extract the longitudinal spin-relaxation times of the ^{83}Kr nuclei for the four cells studied. This measurement was made using cell 3.

$$\frac{\Gamma}{2}\frac{\Delta\nu(^{85}\mathrm{Rb})}{\Delta\nu(^{83}\mathrm{Kr})}=\frac{11}{8}f\left[\gamma_M N_P\frac{P_F}{P_S}\frac{1}{1+br}+2[\mathrm{Kr}]\langle v\sigma\rangle\right], \tag{2}$$

where γ_M, defined by (22) and (23), is a characteristic spin-relaxation rate due to van der Waals molecules, f is the isotopic fraction of ^{83}Kr, [Kr] is the number density of Kr, P_F is the Rb hyperfine polarization defined in (9), P_S is the Rb electronic polarization defined in (11), N_P is a normalization factor defined in (10), and $\langle v\sigma\rangle$ is the velocity averaged binary-spin-exchange cross section defined by (5). Our samples contain mixtures of both Kr and N_2, either of which can act as a third body during molecular formation. The factor $1/(1+br)$ in (2) accounts for the relative importance of N_2 and Kr as third bodies, where $r=P(N_2)/P(\mathrm{Kr})$ is the ratio of the N_2 pressure $P(N_2)$ to the Kr pressure $P(\mathrm{Kr})$. The coefficient $b=P_0(\mathrm{Kr})/P_0(N_2)$, where $P_0(\mathrm{Kr})$ and $P_0(N_2)$ are the characteristic pressures at which the molecular breakup rate τ^{-1} is equal to the spin-rotation frequency $\gamma N/h$ in the limit where only one gas, either the Kr or the N_2, is responsible for the formation and breakup of the van der Waals molecules. The characteristic pressures are defined in (19).

The first term in (2) arises from van der Waals molecules, while the second term arises from binary collisions. The pressure dependence of the two terms is quite different; the first term is proportional to $1/(1+br)$, whereas the second term is proportional to [Kr]. By studying cells that are characterized by various different values of r and [Kr], and fitting our data to (2), we can extract three quantities of interest: γ_M, $\langle v\sigma\rangle$, and $b=P_0(\mathrm{Kr})/P_0(N_2)$. Measurements of $\Delta\nu(^{85}\mathrm{Rb})$, $\Delta\nu(^{83}\mathrm{Kr})$, and Γ were made on each of four cells. The new results reported here, together with earlier measurements by Bouchiat, Brossel, and Pottier,[12] make the spin interaction of the Rb-Kr system the most completely characterized of all the alkali-metal–noble-gas atom pairs.

II. THEORY

To derive (2), we consider the high-pressure short-molecular-lifetime limit defined by

$$\left[\frac{\gamma N\tau}{(2I_i+1)\hbar}\right]^2\ll 1, \tag{3}$$

where I_i is the nuclear spin of one of the two naturally occurring isotopes of Rb. We note that the mean molecular lifetime τ varies inversely with pressure. In this limit, the ratio of the frequency-shift equations (2) and (3) of Ref. 11 have the simple form

$$\frac{\Delta\nu(^{85}\mathrm{Rb})}{\Delta\nu(^{83}\mathrm{Kr})}=\frac{1}{(2I_1+1)}\frac{\langle K_z\rangle}{\langle S_z\rangle}\frac{[^{83}\mathrm{Kr}]}{[\mathrm{Rb}]}, \tag{4}$$

where $[^{83}\mathrm{Kr}]$ is the number density of ^{83}Kr, [Rb] is the number density of rubidium, and $I_1=\frac{5}{2}$ is the nuclear spin of the isotope ^{85}Rb whose EPR frequency is detected.

Next we must derive an expression for $\langle K_z\rangle$. We begin with the rate equation governing the time evolution of $\langle K_z\rangle$, which in the limit (3), is given by Eq. (109) of Ref. 1 which we have generalized to include the effects of binary collisions and wall relaxation:

$$\frac{d}{dt}\langle K_z\rangle=\frac{1}{T_K}\sum_{i=1}^{2}f_i\left[\frac{\alpha\tau}{(2I_i+1)\hbar}\right]^2(\langle\hat{K}^2-K_z^2\rangle\langle F_{iz}\rangle-\langle\hat{F}_i^2-F_{iz}^2\rangle\langle K_z\rangle)$$
$$+[\mathrm{Rb}]\langle v\sigma\rangle(2\langle S_z\rangle\langle\hat{K}^2-K_z^2\rangle-\langle K_z\rangle)-\Gamma'\langle K_z\rangle, \tag{5}$$

where $1/T_K$ is the formation rate of van der Waals molecules per noble-gas atom, and we have introduced the operator $\mathbf{F}$, the total angular momentum of the Rb atom. Also, we have introduced the notation $\hat{F}^2=\mathbf{F}\cdot\mathbf{F}$. The sum in the first term contains two terms corresponding to the two naturally occurring isotopes of rubidium, ^{85}Rb ($I_1=\frac{5}{2}$) and ^{87}Rb ($I_2=\frac{3}{2}$), that occur with isotopic fractions $f_1=0.7215$ and $f_2=0.2785$, respectively. The first term on the right-hand side of (5) describes spin exchange that takes place in van der Waals molecules, the second term describes spin exchange that takes place during binary collisions, and the last term describes spin relaxation due to wall collisions and perhaps magnetic field inhomogeneities.

Under our experimental conditions we expect the Zeeman sublevel populations of the Kr atoms to be in spin temperature equilibrium, so the relative population $\rho(m)$ of sublevels with azimuthal quantum number m will be proportional to $e^{\beta(\mathrm{Kr})m}$, where $\beta(\mathrm{Kr})$ is the spin-temperature parameter. The wall relaxation rate Γ' is always so great compared to the spin-exchange rate of the Kr nuclei with the Rb vapor that $\beta(\mathrm{Kr})\ll 1$. For small values of $\beta(\mathrm{Kr})$ one can readily show that

$$\langle\hat{K}^2-K_z^2\rangle=\tfrac{2}{3}K(K+1)+\mathcal{O}(\beta^2(\mathrm{Kr})), \tag{6}$$

where $\mathcal{O}(\beta^2(\mathrm{Kr}))$ represents terms of order β^2. Using (6), we can write the equilibrium solution of (5) as

$$\langle K_z\rangle=\frac{1}{\Gamma}\left[\frac{1}{T_K}\left[\frac{\alpha\tau}{\hbar}\right]^2\sum_i\frac{f_i\langle F_{iz}\rangle}{(2I_i+1)^2}+2[\mathrm{Rb}]\langle v\sigma\rangle\langle S_z\rangle\right]\tfrac{2}{3}K(K+1), \tag{7}$$

where

$$\Gamma=\Gamma'+[\mathrm{Rb}]\langle v\sigma\rangle+\frac{1}{T_K}\sum_i f_i\left[\frac{\alpha\tau}{(2I_i+1)\hbar}\right]^2\langle\hat{F}_i^2-F_{iz}^2\rangle. \tag{8}$$

Physically, Γ is the relaxation rate of $\langle K_z \rangle$ due to both wall collisions and the Rb vapor, and is measured by taking data of the sort shown in Fig. 2. We note that Γ has a slightly different value when the Kr is being polarized than it does when the Kr polarization is allowed to decay as it is in Fig. 2. This is because Γ depends on the Rb polarization through the last term of (8). In our experimental conditions, however, the second two terms of (8) are at most about 2% of the size of Γ'. This follows from the fact that $\langle K_z \rangle$ is never great than about 2% of its maximum possible value. For instance, of cell 1, we measured $\Gamma = \frac{1}{733}$ sec, and the second two terms of (8) can be computed to be $\frac{1}{41077}$ sec for the case of low Rb polarization. (The second two terms are even smaller for high Rb polarization.) Noting that the second two terms of (8) change by less than a factor of 2 between high and low Rb polarization, we conclude that approximating Γ as being independent of the Rb polarization results in less than a 1% error.

To simplify (7), it is convenient to introduce a hyperfine polarization P_F defined by

$$P_F = \frac{1}{N_P} \sum_i \frac{2 f_i \langle F_{iz} \rangle}{(2I_i+1)^2} , \tag{9}$$

where the hyperfine polarization normalization factor N_P is defined by

$$N_P = \sum_i \frac{f_i}{(2I_i+1)} . \tag{10}$$

For natural Rb, $N_P = 0.1899$. From the definition of P_F it is clear that $-1 \le P_F \le 1$. Similarly, we define an electronic polarization P_S where

$$P_S = 2\langle S_z \rangle . \tag{11}$$

In the limit of high polarization, $|P_F| = |P_S| = 1$. The polarization of the Rb vapor, like the Kr polarization, can be described by a single spin-temperature parameter β(Rb). Consequently, both P_F and P_S are well-defined functions of β(Rb) and one can use some of the arguments presented in Ref. 1 to show that

$$\lim_{\beta(\mathrm{Rb}) \to 0} P_F / P_S = \frac{1}{N_P} \sum_i \frac{1 + \frac{4}{3} I_i (I_i+1)}{(2I_i+1)^2} f_i = 1.887 , \tag{12}$$

where the numerical value is for natural Rb. Thus the ratio P_F/P_S is bounded between 1 and 1.887, which is important for the interpretation of our experimental results. In terms of P_F, P_S, and N_P, we can write $\langle K_z \rangle$ as

$$\langle K_z \rangle = \frac{1}{\Gamma} \left[\frac{1}{T_K} \left(\frac{\alpha \tau}{\hbar} \right)^2 \tfrac{1}{2} N_P P_F + [\mathrm{Rb}] \langle v \sigma \rangle P_S \right] \tfrac{2}{3} K (K+1) . \tag{13}$$

Our experimental samples contain both Kr and N_2, and either gas can act as a third body during the formation and breakup of the van der Waals molecules. In order to most simply take this fact into account, we notice that in Eq. (5), the molecular contribution to spin exchange is proportional to τ^2/T_K. In chemical equilibrium the breakup rate of molecules per unit volume must equal the formation rate per unit volume and we must therefore have

$$\frac{[\mathrm{Rb\text{-}Kr}]}{\tau} = \frac{[\mathrm{Kr}]}{T_K} = \frac{[\mathrm{Rb}]}{T_F} , \tag{14}$$

where [Rb-Kr] is the number density of van der Waals molecules, and $1/T_F$ is the formation rate of van der Waals molecules per alkali-metal atom. From (14) we have that

$$\frac{1}{T_F} = [\mathrm{Kr}] \kappa \tau^{-1} , \tag{15}$$

where κ is the chemical equilibrium constant:

$$\kappa = \frac{[\mathrm{Rb\text{-}Kr}]}{[\mathrm{Rb}][\mathrm{Kr}]} . \tag{16}$$

From (15) it follows that

$$\frac{1}{T_F} \left(\frac{\alpha \tau}{\hbar} \right)^2 = [\mathrm{Kr}] \kappa \tau \left(\frac{\alpha}{\hbar} \right)^2 . \tag{17}$$

The molecular breakup rate $1/\tau$ can be written as the sum of two terms corresponding to breakup due to collisions with Kr atoms and N_2 molecules, respectively. Thus

$$\frac{1}{\tau} = \left(\frac{1}{\tau} \right)_{\mathrm{Kr}} + \left(\frac{1}{\tau} \right)_{\mathrm{N_2}} . \tag{18}$$

The characteristic pressure P_0 is defined by the equation

$$\tau = \frac{\hbar}{\gamma N} \frac{P_0}{P} , \tag{19}$$

from which it follows that

$$\frac{1}{\tau} = \frac{\gamma N}{\hbar} \left[\frac{P(\mathrm{Kr})}{P_0(\mathrm{Kr})} + \frac{P(\mathrm{N_2})}{P_0(\mathrm{N_2})} \right] = \frac{\gamma N}{\hbar} \frac{P(\mathrm{Kr})}{P_0(\mathrm{Kr})} (1 + br) , \tag{20}$$

where b and r were defined earlier. Substituting (20) into (17) we get that

$$\frac{1}{T_F} \left(\frac{\alpha \tau}{\hbar} \right)^2 = [\mathrm{Kr}] \kappa \frac{\hbar}{\gamma N} \frac{P_0(\mathrm{Kr})}{P(\mathrm{Kr})} \frac{1}{1+br} \left(\frac{\alpha}{\hbar} \right)^2 = \gamma_M \frac{1}{1+br} , \tag{21}$$

where

$$\gamma_M = \lim_{P(\mathrm{N_2}) \to 0} \frac{1}{T_F} \left(\frac{\alpha \tau}{\hbar} \right)^2 . \tag{22}$$

From the ideal-gas law we know that $P(\mathrm{Kr}) = [\mathrm{Kr}] k_B T$, which when substituted into (21) allows us to express

$$\gamma_M = \frac{\kappa \hbar P_0(\mathrm{Kr})}{\gamma N k_B T} \left(\frac{\alpha}{\hbar} \right)^2 , \tag{23}$$

which is independent of Kr pressure, and is thus fundamental to the Rb-Kr system. Physically, γ_M is the spin-relaxation rate of hypothetical rubidium atoms with nu-

clear spin $I=0$, due to the interaction $\alpha \mathbf{K}\cdot\mathbf{S}$ in Rb-Kr van der Waals molecules when the Rb atoms are in pure ^{83}Kr gas at sufficiently high pressure that the molecular contributions to Rb spin-relaxation rate have saturated.

We note that γ_M is related in a simple way to the quantity $\mathfrak{a}^*$, which Bouchiat defined as the high-pressure low-magnetic-field limit of the slowest spin-relaxation rate of alkali-metal atoms due to alkali-metal–noble-gas van der Waals molecules.[12] Bouchiat showed that

$$\mathfrak{a}_i^* = \frac{2}{3}\frac{1}{T_F}\frac{1}{(2I_i+1)^2}\left[\frac{\gamma N \tau}{\hbar}\right]^2 , \tag{24}$$

where the subscript i refers to the specific isotope of Rb whose spin relaxation is being studied. We note that this expression ignored the Rb spin relaxation due to nonzero noble-gas nuclear spin, which in Bouchiat's measurement was a small effect. Bouchiat's measurements were made with samples that contained alkali-metal atoms and noble-gas atoms, without the presence of N_2 as in our measurements. We can relate $\mathfrak{a}_i$ to γ_M through the quantity

$$x = \gamma N/\alpha , \tag{25}$$

the ratio of the strength of the spin-rotation interaction to the Fermi-contact interaction. The quantity x has been discussed extensively elsewhere,[1,2] and is very useful for characterizing alkali-metal–noble-gas systems. Later, we will extract a value for x from our measurements. Using (22) and (25) we have that

$$\gamma_M = \left[\tfrac{1}{2}(2I_i+1)^2\frac{1}{x^2}\right]\mathfrak{a}_i^* . \tag{26}$$

Returning to our derivation, we express the factor $(1/T_K)(\alpha\tau/\hbar)^2$, which depends on both the Kr pressure and the N_2 pressure, in terms of γ_M with the help of (14) and (21):

$$\frac{1}{T_K}\left[\frac{\alpha\tau}{\hbar}\right]^2 = \frac{[\mathrm{Rb}]}{[\mathrm{Kr}]}\frac{1}{T_F}\left[\frac{\alpha\tau}{\hbar}\right]^2 = \frac{[\mathrm{Rb}]}{[\mathrm{Kr}]}\gamma_M\left[\frac{1}{1+br}\right] . \tag{27}$$

Substituting (27) into (13) we obtain

$$\langle K_z\rangle = \frac{1}{\Gamma}\left[\frac{[\mathrm{Rb}]}{[\mathrm{Kr}]}\gamma_M \tfrac{1}{2}N_P P_F\left[\frac{1}{1+br}\right] + [\mathrm{Rb}]\langle v\sigma\rangle P_S\right]\tfrac{2}{3}K(K+1) . \tag{28}$$

Substituting (28) into (4), and inserting the numerical values $I_1=\frac{5}{2}$ and $K=\frac{9}{2}$, we arrive finally at (2).

III. EXPERIMENT

A schematic of some of the key components of the experimental apparatus is shown in Fig. 3. Measurements are made on sealed Pyrex cells that contain krypton, isotopically enriched to a fraction of 0.70 ± 0.01 ^{83}Kr, nitrogen, and several milligrams of natural rubidium. The cells are contained in an oven and heated to a temperature of 90 °C to achieve a Rb number density of about 3×10^{12} cm^{-3}. A static magnetic field of 0.11 G is produced by a solenoid. Magnetic shielding is used to reduce magnetic noise to less than 1 mG, and a Cs magnetometer not shown in Fig. 3 is used to sense the magnitude of the field. Any fluctuations in the field are canceled by feedback of current into the compensating coils shown in Fig. 3.

The frequency shifts of the alkali-metal EPR lines are measured by using a feedback system to actively lock a voltage-controlled oscillator (VCO) to the 100th harmonic of the EPR frequency of ^{85}Rb. The EPR frequency is determined by measuring the VCO frequency with a gated counter. This technique is described in greater detail in Ref. 11. A measurement of $\Delta\nu(^{85}\mathrm{Rb})$ consists of three phases. In the first phase the cell is subjected to a strong inhomogeneous oscillating magnetic field at the Larmor frequency of the krypton. This ensures that no polarization exists in the krypton.[13,14] During the next phase, the Rb atoms in the vapor phase are maintained at high polarization by optical pumping with several hundred milliwatts of circularly polarized 794.8-nm light from a cw

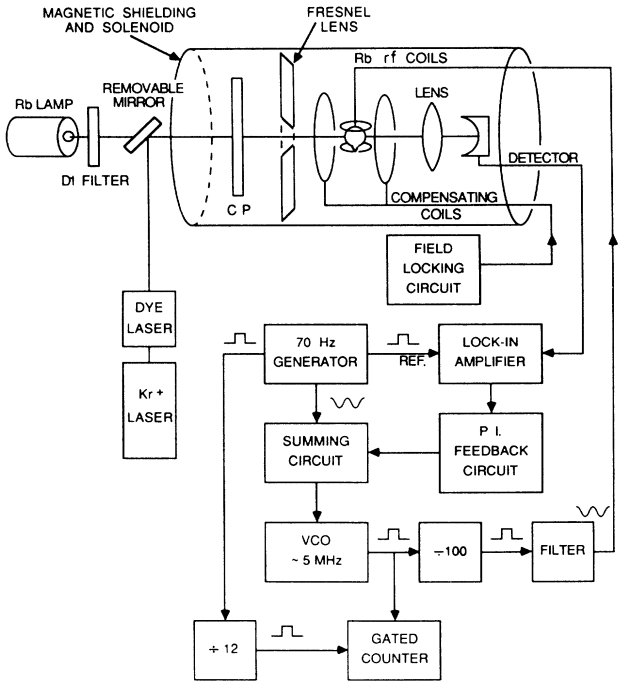

FIG. 3. Schematic diagram of the experimental apparatus emphasizing the components used for locking to the EPR frequency of the Rb. An error signal from the lock-in amplifier is fed through a proportional and integral (P.I.) feedback circuit and a summing circuit to lock the voltage-controlled oscillator (VCO) onto the 100th harmonic of the Rb EPR line. Not shown are the coils used to produce the oscillating field used during the NMR scans, or the Cs magnetometer and other components used to lock the magnetic field.

dye laser, pumped by a krypton-ion laser. During the pumping phase, angular momentum is transferred from the spin-polarized Rb atoms to the nuclear spins of the ^{83}Kr atoms in spin-exchange collisions and in van der Waals molecules. The final phase consists of observing the EPR frequency shift in the Rb metal due to the nuclear polarization of the krypton. The EPR shift decays with time, thereby providing a measure of the longitudinal spin-relaxation rate Γ, as is illustrated in Fig. 2.

The determination of $\Delta\nu(^{83}\mathrm{Kr})$ relies on techniques identical to those used for the measurement of $\Delta\nu(^{85}\mathrm{Rb})$ except that during the pumping phase an oscillating magnetic field is applied to the ^{83}Kr. When the frequency of the oscillating field is near the Larmor frequency of the krypton atoms, the buildup of polarization is inhibited because of the precession of the krypton atoms. The shift of the Rb EPR frequency at the end of the pumping phase is proportional to the polarization that has built up in the krypton. An NMR line is measured by making a series of measurements of $\Delta\nu(^{85}\mathrm{Rb})$, each of which corresponds to a different frequency of the oscillating field that is applied during the pump-up phase. A representative measurement of the frequency shift of the NMR lines of the krypton is shown in Fig. 1. Both NMR lines correspond to the ground-state Zeeman splitting in ^{83}Kr. Measured in the presence of polarized alkali vapor, the two NMR lines correspond to the alkali spin oriented parallel and antiparallel to the external magnetic field. The separation of the two NMR lines is equal to $2\Delta\nu(^{83}\mathrm{Kr})$.

Measurements were made on four sample cells. The contents of each cell, together with the measured values for $\Delta\nu(^{85}\mathrm{Rb})$, $\Delta\nu(^{83}\mathrm{Kr})$, and Γ, are given in Table I. A least-squares fit of the data of Table I to Eq. (2) is illustrated in Fig. 4. The upper curve corresponds to a krypton pressure of 25 Torr, and the bottom curve corresponds to a krypton pressure of 15 Torr. The base line that is drawn is the fitted binary contribution to the data corresponding to a krypton pressure of 15 Torr, and is thus the asymptote for the lower curve. Three quantities can be extracted from the fit of our data to (2): the velocity-averaged binary spin-exchange cross section $\langle v\sigma\rangle$, the characteristic molecular spin-relaxation rate γ_M, and the ratio $P_0(\mathrm{Kr})/P_0(\mathrm{N_2})$, shown as items (1)–(3) in Table II.

In order to determine γ_M we must know, for each cell, the ratio of the Rb hyperfine polarization to the Rb electronic polarization P_F/P_S. The noble-gas NMR frequency shift is given by

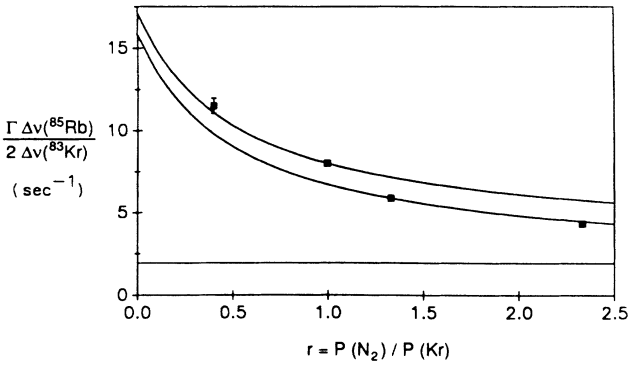

FIG. 4. The data contained in Table I are graphed as a function of $r=P(\mathrm{N_2})/P(\mathrm{Kr})$, together with a fit to Eq. (2). Three quantities are extracted from the fit: the velocity-averaged binary spin-exchange cross section $\langle v\sigma\rangle$, the ratio $b=P_0(\mathrm{Kr})/P_0(\mathrm{N_2})$, and the characteristic spin-relaxation rate γ_M due to van der Waals molecules. The fitted values for $\langle v\sigma\rangle$, γ_M, and b are shown as items (1), (2), and (3) of Table I. The upper curve corresponds to cells 3 and 4, each of which contains 25 Torr of Kr. The lower curve corresponds to cells 1 and 2, each of which contains 15 Torr of Kr. The displacement of the two curves yields a measure of $\langle v\sigma\rangle$.

$$2\Delta|\nu(^{83}\mathrm{Kr})|=-\frac{1}{h}\frac{|\mu_{\mathrm{Kr}}|}{K}\frac{8\pi}{3}\mu_B g_S\kappa_0[\mathrm{Rb}]P_S\ , \qquad (29)$$

where μ_{Kr} is the magnetic moment of ^{83}Kr, μ_B is the Bohr magneton, g_S is the Landé g factor, and $\kappa_0=270\pm95$ is an enhancement factor, specific to the Rb-Kr system, that has been measured previously by Schaefer *et al.*[11,15] The knowledge of κ_0 provides a calibration enabling us to use (29) to relate $\Delta\nu(^{83}\mathrm{Kr})$ to the Rb electronic polarization P_S for each cell measured. Because of the spin-temperature equilibrium in the Rb vapor, a determination of P_S is equivalent to a determination of the spin-temperature parameter $\beta(\mathrm{Rb})$, from which P_F and P_F/P_S can be computed. As discussed in connection with (12), the ratio P_F/P_S is constrained to lie between 1 at high polarization and 1.887 at low polarization. While P_S is only known absolutely to about 33% because of uncertainties in κ_0, the bounded ratio P_F/P_S is known much better. For the four cells measured, P_S ranged between 0.57 and 0.74, and the ratio P_F/P_S ranged between 1.15 and 1.28. The average value of P_F/P_S for the four cells used in our measurements was

TABLE I. Experimental measurements.

Cell No.	$P(\mathrm{Kr})$ (torr)	$P(\mathrm{N_2})$ (torr)	$1/\Gamma$ (sec)	$\Delta\nu(^{85}\mathrm{Rb})$ (Hz)	$2\Delta\nu(\mathrm{Kr})$ (mHz)	$\frac{\Gamma\Delta\nu(^{85}\mathrm{Rb})}{2\Delta\nu(^{83}\mathrm{Kr})}$ (sec^{-1})
1	15	20	733±5	49.4±1.0	11.48±0.10	5.87±0.13
2	15	35	872±5	48.5±1.0	12.82±0.10	4.34±0.11
3	25	10	466±3	52.9±2.0	9.85±0.10	11.52±0.46
4	25	25	605±4	59.9±1.5	12.34±0.15	8.02±0.22

TABLE II. Summary of results.

(1)	$\langle v\sigma \rangle$	$(2.1\pm0.5)\times10^{-18}$ cm^3 sec^{-1}	fitted
(2)	γ_M	63 ± 12 sec^{-1}	fitted
(3)	$P_0(\mathrm{Kr})/P_0(\mathrm{N_2})$	1.90 ± 0.54	fitted
(4)	$T_F P^2$	$(1.06\pm0.05)\times10^{-2}$ sec Torr^2	Ref. 12
(5)	τP	$(5.69\pm0.17)\times10^{-8}$ sec Torr	Ref. 12
(6)	$\gamma N/h$	26.85±0.78 MHz	Ref. 12
(7)	$P_0(\mathrm{Kr})$	9.60±0.40 Torr	Ref. 12
(8)	$(\tau^2/T_F)_{\mathrm{Kr}}$	$(20.8\pm1.6)\times10^{-14}$ sec	From items (4) and (5), adjusted for temperature.
(9)	α/h	2.77±0.27 MHz	From items (2) and (8).
(10)	$x=\gamma N/\alpha$	9.68±0.95	From items (6) and (8).
(11)	$P_0(\mathrm{N_2})$	5.1±1.4 Torr	From items (3) and (10).

1.20±0.12, which is used in the plot shown in Fig. 4. In deriving the fitted value of γ_M that is quoted as item (2) of Table II, we have taken into account the small cell-to-cell variations of P_F/P_S.

Several quantities of interest can be obtained by comparing our measurements with the measurements, described in Ref. 12, that were made by Bouchiat, Brossel, and Pottier. The strength of the Fermi contact interaction α can be deduced from our determination of γ_M if we know τ^2/T_F. We use Bouchiat's measurements of $T_F P^2$ and τP, which are listed in Table II as items (4) and (5), to derive $\tau^2/T_F = 30.54\times10^{-14}$ sec. Bouchiat's measurements were made in the absence of N_2, at 27 °C. Our measurements were performed at 90 °C, so we must scale τ^2/T_F to account for the temperature difference. We assume that $1/\tau \propto T^{1/2}$, where T is the temperature. This follows if we assume that the breakup cross section is nearly velocity independent. The temperature dependence of $1/T_F$ follows from considering (15). If we assume that the van der Waals potential is shallow enough that the Boltzmann factor $e^{-V/kT}$ does not vary much from unity, then $\kappa \propto T^{-3/2}$ because of the temperature dependence of the phase space of an ideal gas. Since $1/T_F \propto \kappa\tau^{-1}$, it follows that $1/T_F \propto 1/T$. We conclude that $\tau^2/T_F \propto 1/T^2$, which we have used to arrive at the temperature scaled value that is listed as item (8) in Table II. Using τ^2/T_F and our measured value of γ_M, we arrive at the value of α/h that is listed as item (9).

Another quantity of interest is the ratio $x=\gamma N/\alpha$. Using Bouchiat's measurement of γN, we can calculate the ratio $x=\gamma N/\alpha$, which is given as item (10) in Table II. It is important to note that γN is expected to vary by less than 1% in the temperature range spanned by Bouchiat's measurements and ours.[16] The physical reason for this is due primarily to two things. Firstly, the population distribution of the angular momentum states of the van der Waals molecules depends only weakly on temperature. Secondly, the spin-rotation coupling constant γ depends only weakly on temperature. The temperature dependence of the spin-rotation coupling constant γ arises from the dependence of γ on the interatomic distance R (see Ref. 17). The positions of the minima of the effective potential curves for the van der Waals molecules determine R, and the minima change only slightly as a function of N. Thus the fact that N depends only slightly on temperature greatly suppresses any temperature dependence that γ might have.

Finally, using Bouchiat's measurement of $P_0(\mathrm{Kr})$, we can use our measured value of $P_0(\mathrm{Kr})/P_0(\mathrm{N_2})$ to calculate $P_0(\mathrm{N_2})$, which is given as item (11). We note that from (19), P_0 depends on the product $\tau\gamma N$. Since γN is largely independent of temperature, and $\tau \propto T^{-1/2}$, we expect $P_0 \propto T^{-1/2}$. Bouchiat's measurements of $P_0(\mathrm{Kr})$ were made at 27 °C, and we have not applied any temperature scaling, so our quoted value of $P_0(\mathrm{N_2})$ is for a temperature of 27 °C.

IV. CONCLUSIONS

We can summarize our results as follows.

(1) We have determined, for the first time, the parameters that govern the polarization of ^{83}Kr nuclei through their interaction with optically pumped Rb vapor.

(2) It is interesting to compare some of the experimentally determined parameters that are summarized in Table II with some recent estimates that have been calculated by Walker.[16] As is shown in Table III, the agreement is quite good, particularly given the fact that Walker's estimates were not meant to be extremely precise.

(3) The study of the ratio of frequency shifts is an important new technique for studying spin-exchange parameters in alkali-metal–noble-gas systems. It is particularly useful when temperature-dependent wall relaxation effects complicate measurements in which the Rb number density is temperature controlled.

(4) At high pressures, where spin exchange is dominated by binary collisions, the ratio of frequency shifts does not depend on the Rb polarization, and the binary spin-

TABLE III. Comparison with calculations.

Quantity	Calculated (Ref. 16)	Experimental (See Table II)
σ	7.1×10^{-7} Å^2	$(4.9\pm1.2)\times10^{-7}$ Å^2
$\gamma N/h$	21 MHz	26.85±0.78 MHz
α/h	1.8 MHz	2.77±0.27 MHz
$x=\gamma N/\alpha$	11.7	9.68±0.95

exchange cross section could be measured with an accuracy of several percent or less. Also, as the enhancement parameters κ_0 for various different alkali-metal–noble-gas pairs are determined with better precision, the use of frequency shifts at lower pressures will yield more accurate results.

ACKNOWLEDGMENTS

We would like to acknowledge many useful conversations with Thad Walker. This work was supported by the U.S. Air Force Office of Scientific Research under Grant No. 88-0165.

[1]W. Happer, E. Miron, S. Schaefer, D. Schrieber, W. A. van Wijngaarden, and X. Zeng, Phys. Rev. A **29**, 3092 (1984).

[2]X. Zeng, Z. Wu, T. Call, E. Miron, D. Schreiber, and W. Happer, Phys. Rev. A **31**, 260 (1985).

[3]Z. Wu, W. Happer, and J. M. Daniels, Phys. Rev. Lett. **59**, 1480 (1987).

[4]T. E. Chupp, R. J. Hoare, R. A. Loveman, E. R. Oteiza, J. M. Richardson, M. E. Wagshul, and A. K. Thompson, Phys. Rev. Lett. **63**, 1541 (1989).

[5]T. G. Vold, F. Raab, B. Heckel, and E. N. Fortson, Phys. Rev. Lett. **52**, 2229 (1984).

[6]F. P. Calaprice, W. Happer, D. F. Schreiber, M. M. Lowry, E. Miron, and X. Zeng, Phys. Rev. Lett. **54**, 174 (1985); M. Kitano, M. Bourzutschky, F. P. Calaprice, J. Clayhold, W. Happer, and M. Musolf, Phys. Rev. A **34**, 1974 (1986); M. Kitano, F. P. Calaprice, M. L. Pitt, J. Clayhold, W. Happer, M. Kadar-Kallen, M. Musolf, G. Ulm, K. Wendt, T. Chupp, J. Bonn, R. Neugart, E. Otten, and H. T. Duong, Phys. Rev. Lett. **60**, 2133 (1988).

[7]T. E. Chupp, M. E. Wagshul, K. P. Coulter, A. B. McDonald, and W. Happer, Phys. Rev. C **36**, 2244 (1987); O. Hausser *et al.*, TRIUMF (unpublished); O. Hausser *et al.*, TRIUMF (unpublished); R. Milner *et al.* (unpublished).

[8]K. P. Coulter, T. E. Chupp, A. B. McDonald, C. D. Bowman, J. D. Bowman, J.J. Szymanski, V. Yuan, G. D. Cates, D. R. Benton, and E. D. Earle, Nucl. Instrum. Methods **A288**, 463 (1990).

[9]Souder *et al.* (unpublished).

[10]B. C. Grover, Phys. Rev. Lett. **40**, 391 (1978).

[11]S. R. Schaefer, G. D. Cates, Ting-Ray Chien, W. Happer, and T. G. Walker, Phys. Rev. A **39**, 5613 (1989).

[12]M. A. Bouchiat, J. Brossel, and L. C. Pottier, J. Chem. Phys. **56**, 3703 (1972).

[13]G. D. Cates, S. Schaefer, and W. Happer, Phys. Rev. A **37**, 2877 (1988).

[14]G. D. Cates, D. J. White, Ting-Ray Chien, S. R. Schafer, and W. Happer, Phys. Rev. A **38**, 5092 (1988).

[15]S. R. Schaefer, Ph.D. thesis, Princeton University, 1988.

[16]Thad G. Walker, Phys. Rev. A **40**, 4959 (1989); also by private communication.

[17]Z. Wu, T. G. Walker, and W. Happer, Phys. Rev. Lett. **54**, 1921 (1985)